

# Chemical Composition Effect of Sol-Gel Derived Bioactive Glass Over Bioactivity Behavior

L.A. Quintero and D.M. Escobar

**Abstract** Bioactive glasses (BG) are a group of inorganic materials widely used in Bone Tissue Engineering (BTE). These biomaterials react with body fluids resulting in the formation of bone like apatite layer. In this study, sol-gel derived bioactive glass was synthesized in the  $\text{SiO}_2\text{-CaO-P}_2\text{O}_5$  system according to augmented constrained mixture experimental design, with percentage restrictions for each oxide as follows:  $58 \leq \text{SiO}_2 \leq 70$ ;  $6 \leq \text{P}_2\text{O}_5 \leq 9$  and  $24 \leq \text{CaO} \leq 34$ . BG were conformed into short-bulk cylinders and immersed in Simulated Body Fluid (SBF) solution for 7 and 14 days in order to carry out bioactivity tests. Apatite layer formation was confirmed by Scanning Electron Microscopy (SEM) and Energy Dispersive X-ray Analysis (EDX). The results showed apatite layer formation depended on BG chemical composition proved with  $p$ -values from ANOVA analysis below 0.05 indicating factors significance over the response. The formed apatite layer presented a Ca/P ratio similar to bone apatite, this result is appropriate for biomaterials used in BTE.

**Keywords** Bioactive glasses · Apatite layer · Bone tissue engineering · SBF

## Introduction

Bioactive glasses (BG) are a group of bio-ceramics based on silicon oxide which have been used due to their excellent bioactivity that increases apatite layer formation allowing a suitable and safe chemical bond between the material and living bone [1]. The formed apatite layer on the surface of BG in presence of simulated body fluid (SBF) is similar to that of the mineral phase present in the bone [2]. It has been proved that BG dissolution products could stimulate cell proliferation and

---

L.A. Quintero (✉) · D.M. Escobar  
Biomaterials Research Group, Engineering Faculty,  
University of Antioquia, St 70 N° 52-21, Medellin, Colombia  
e-mail: lindsey.alejandra@gmail.com

© The Minerals, Metals & Materials Society 2017  
M.A. Meyers et al. (eds.), *Proceedings of the 3rd Pan American Materials Congress*,  
The Minerals, Metals & Materials Series, DOI 10.1007/978-3-319-52132-9\_2

differentiation that eventually can promote new bone formation and, according to silicon oxide quantity, bone formation is faster with a BG implant than synthetic hydroxyapatite [3, 4].

Most used BG is 45S5 Bioglass<sup>®</sup> first reported by Larry Hench [5] and obtained through melting-quenching process. However, this process requires higher temperatures and limits porosity, particle size and specific surface of final powder [6]. An alternative synthesis route is sol-gel process, a technique used since early 90s. Sol-gel synthesis provides powder with lower crystallinity, different morphologies and is more versatile than melt method [2].

Within the glass and glass-ceramic systems,  $\text{SiO}_2\text{-CaO-P}_2\text{O}_5$  has been considered as a base system to include new formulations and molar proportions of oxides [7]. These proportions have been conventionally defined through laborious practices as trial-and-error methods, in which many resources are expended. Therefore, the use of more sophisticated statistical methodologies as Mixture Experimental Designs (MED) could be a useful tool to determinate a suitable bioactivity behavior from the control of main oxides for the BG synthesis. Statistical softwares provide the experimental region conformed to provided restrictions consistent with constrained mixture design (CMD) theoretical equations [8].

Bioactivity behavior, it can be measured through bioactive tests according to reported by Kokubo et al. [9] by submerging the material in SBF. BG in presence of SBF ions can form a bone like apatite layer, especially those obtained by sol-gel techniques due to  $\text{OH}^-$  groups on their surface, which are able to induce Hydroxyapatite nucleation [2]. There are diverse chemical and physical procedures to evaluate the formed apatite layer, such as Fourier Transformed InfraRed (FTIR), X-ray Diffraction (XRD), Scanning Electron Microscopy (SEM), Energy Dispersive X-ray (EDX), among others.

In this study, BG was synthesized according to an augmented constrained mixture design to establish the best conditions in a highly bioactive BG for BTE applications. The percentage of formed apatite layer was measured through SEM analysis and the stoichiometric ratios of that layer, namely Ca/P ratio near to natural ratio, was measured with EDX several times in similar places to determine a point of comparison.

## Materials and Methods

### *Materials*

Tetraethylorthosilicate (TEOS:  $\text{C}_8\text{H}_{20}\text{O}_4\text{Si}$ ) and Calcium Acetate (CaAc:  $\text{Ca}(\text{CH}_3\text{COO})_2$ ) were purchased from Merck Inc; Ammonium Dihydrogen Phosphate (ADP:  $\text{NH}_4\text{H}_2\text{PO}_4$ ) was purchased from Carlo Erba Reagent; Ethanol was purchased from Panreac. All chemicals from SBF preparation were provided from Sigma-Aldrich, Germany.

## Mixture Experimental Design

In this study an analysis of variance (ANOVA) based on an augmented CMD was used to evaluate the effect of molecular fraction of  $\text{SiO}_2$  ( $X_1$ ),  $\text{P}_2\text{O}_5$  ( $X_2$ ) and  $\text{CaO}$  ( $X_3$ ) on quantity and quality of formed apatite layer. Based on CMD, the samples were prepared by mixing the three components at different ratios with the summation of the proportions ( $X_1 + X_2 + X_3$ ) one. The restrictions for each oxide were selected according to percentages reported by different authors [7, 10] ( $58 \leq \text{SiO}_2 \leq 70$ ;  $6 \leq \text{P}_2\text{O}_5 \leq 9$  and  $24 \leq \text{CaO} \leq 34$ ). Samples codes and molecular fraction of each experimental point as 10 combinations are showed in Table 1. Experimental points of compositions were defined through R software with mixexp package, which allows to determine the experimental region showed in Fig. 1. The experiments were performed in triplicates of the mixtures, for a total of 30 samples evaluated.

The selected model for ANOVA test was a special cubic model presented in Eq. 1, where  $Y$  is the response,  $\beta_i$  are the constants for each interaction and  $X_i$  are the variables

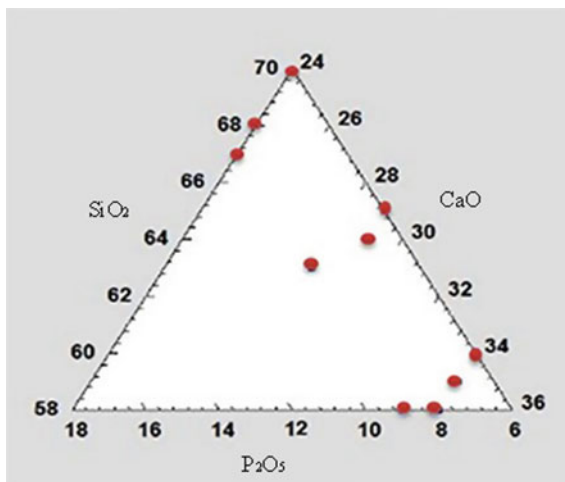
$$Y = \beta_1X_1 + \beta_2X_2 + \beta_3X_3 + \beta_{12}X_1X_2 + \beta_{13}X_1X_3 + \beta_{23}X_2X_3 + \beta_{123}X_1X_2X_3 \quad (1)$$

Fisher's LEAST SIGNIFICANCE DIFFERENCE (LSD) test was performed to determine significant effects of the variables. The chosen significance level was 5% which correspond  $p$ -value = 0.05. The  $p$ -values below 0.05 indicated the statistical significance of the factors.

**Table 1** Molecular fraction of BG components based on CMD

Sample code	Molecular fraction		
	$\text{SiO}_2$	$\text{P}_2\text{O}_5$	$\text{CaO}$
BG1	0.67	0.09	0.24
BG2	0.68	0.08	0.24
BG3	0.58	0.09	0.33
BG4	0.64	0.07	0.29
BG5	0.58	0.08	0.34
BG6	0.70	0.06	0.24
BG7	0.60	0.06	0.34
BG8	0.63	0.09	0.28
BG9	0.59	0.07	0.34
BG10	0.65	0.06	0.29

**Fig. 1** Experimental region of CMD obtained with R software



### ***Bioactive Glass Synthesis***

Sol-gel derived BG was synthesized by dissolving TEOS into an ethanol/distilled water solution, with a molar ratio 1:4 both TEOS/distilled water and TEOS/ethanol according to Vaid et al. [10]. The mixture was left in agitation. ADP and ethanol/distilled water solution with a molar ratio 1:4 both ADP/distilled water and ADP/ethanol were added after 1 h to react completely in stirring for another 45 min. Subsequently, calcium acetate was added to react for 11 min. Finally, an acetic acid/distilled water solution (6:1) was added into mixture (distilled water/BG 1:4). The final solution was kept in agitation until gel point.

BG gel was kept in a container for 3 days at room temperature. The gel was heated at 120 °C for 2 days to remove all water content. Followed by a final mash to obtain a dry powder.

### ***Sample Characterization***

Every synthesized BG was analyzed by X-ray diffraction (XRD) with XPert PANalytical Empyrean Series II diffractometer after thermal treatment at a final temperature of 1050 °C. This instrument worked with voltage and current settings of 45 kV and 40 mA respectively and used  $\text{Cu-K}\alpha$  radiation (1.5405980 Å).

## *In Vitro Bioactivity Study*

The SBF solution was prepared according to Kokubo et al. [9]. BG powder was uniaxially pressed at 30 MPa for 2 min in order to obtain cylindrical disks. The cylinders were immersed in the SBF solution and incubated at 37 °C in close tubes for 7 and 14 days. Afterwards, the cylinders were removed from the SBF solution and washed with distilled water to removed undissolved salts. Finally they were analyzed by Scanning Electron Microscopy (SEM) using a microscope JOEL-JSM 6490 LV that operated at the acceleration voltage of 20 kV. Energy dispersive X-ray (EDX) was performed on the same equipment.

## Results and Discussion

### *XRD Analysis of the Synthesized BG*

Figure 2 presents XRD results for all 10 different BG with narrow and differentiable peaks due to augmented crystallinity with thermal treatment. Figure 2a shows from BG1 to BG5 and Fig. 2b from BG6 to BG10. Primary and secondary peaks in all synthesized BG present consistencies regarding angle and intensity according with reported for comparable systems [4, 11]. Peaks at  $2\theta = 30.9$  and  $21.3$  are primary and secondary peaks for  $\text{SiO}_2$ , respectively. Peaks at  $2\theta = 34.4$  and  $31.3$  are primary and secondary for  $\text{CaO}$ ; and peaks at  $2\theta = 27.7$  and  $25.7$  are primary and secondary for  $\text{P}_2\text{O}_5$ . Those peaks are present in all DRX spectrum; however, BG1, BG2, BG3, BG4, BG8 and BG10 spectra show some other peaks (more than two) possibly due to the formation of undesirable phases, as for BG5, BG6 and BG9 spectra have one or two peaks of other phases, possible pseudo-wollastonites which tend to form with same oxides. BG7 shows no undesirable peaks.

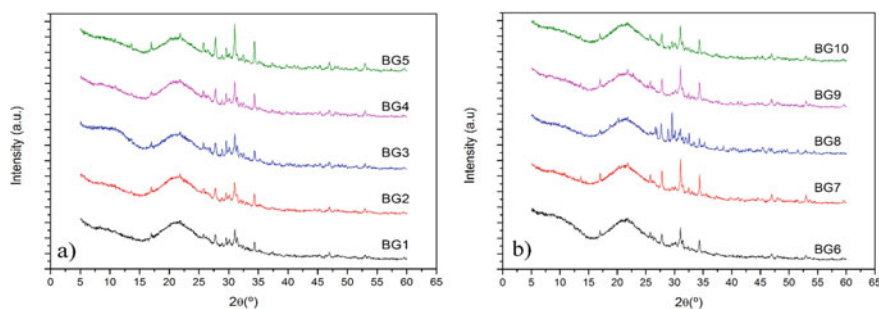


**Fig. 2** XRD patterns of synthesized BG after 1050 °C treatment. **a** BG1 to BG5; **b** BG6 to BG10

### Sample Characterization After In Vitro Tests

Apatite layer formed on the surface of BG cylinders after in vitro tests were analyzed with SEM images and EDX analysis both for 7 and 14 days of study. Figure 3 shows SEM micrographs for each BG, it can be seen that for some of the cylinders the formed apatite layer on their surface decreased with time, which means that the layer is unstable and not desirable for BTE.

On the other hand, the formed layer exhibits a small morphology size as shown in Fig. 4 for the apatite layer on the surface of BG7 at 14 days of study. A small particle size is advantageous since the natural apatite is micro and nano-size [12, 13].

Figures 5 and 6 summarizes Ca/P ratio results and apatite layer percentage (ALP) for synthesized BG after in vitro test. ALP was obtained through image analysis with ImageJ software. Data were collected in triplicate and those results were used to perform statistical analysis with R software.

Statistical results showed that the selected model fits the data ( $R^2 = 0.98$ ), this means that it is possible to analyze the behavior of apatite layer percentage knowing the BG composition.

The Ca/P ratio results showed that according to BG compositions, the formed apatite layer can be similar of natural hydroxyapatite, which varies between 1.37 and 1.87 [13] indicating the appropriate results for BG5 and BG7 obtained after 14 days of SBF immersion. From Fig. 6 is observed two different tendencies for

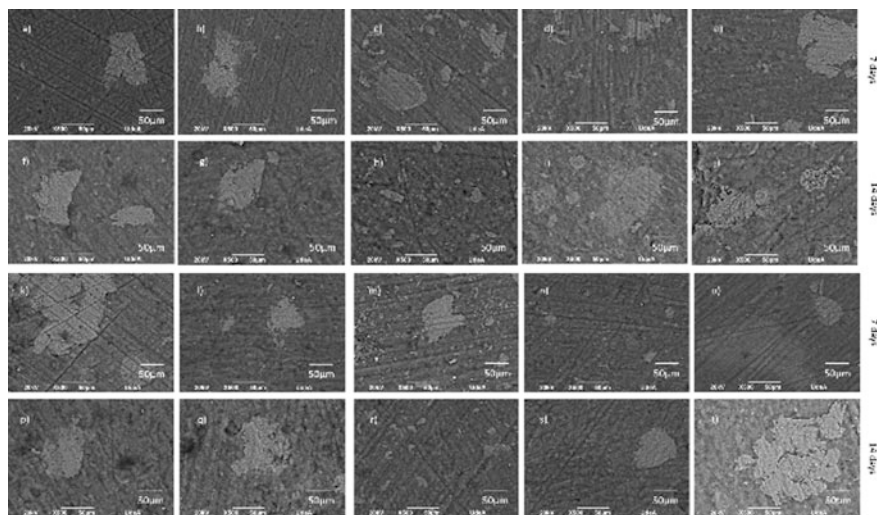


**Fig. 3** SEM micrographs of synthesized BG after SBF immersion. **a** and **f** are SEM images for BG1 after 7 (**a**) and 14 (**f**) of immersion; **b** and **g** are for BG2; **c** and **h** are for BG3; **d** and **i** are for BG4; **e** and **j** are for BG5; **k** and **p** are for BG6; **l** and **q** are for BG7; **m** and **r** are for BG8; **n** and **s** are for BG9; **o** and **t** are for BG10

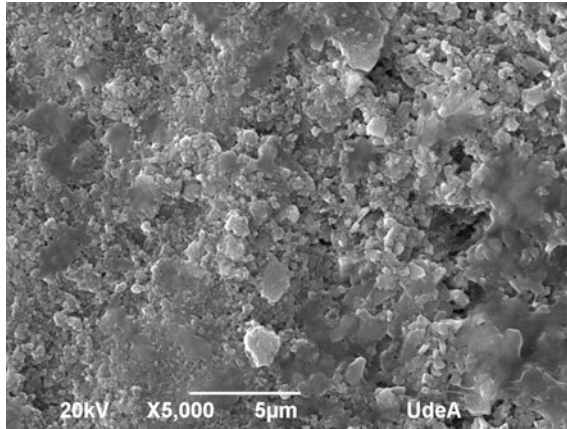


**Fig. 4** SEM micrograph of formed apatite layer for BG7 after 14 days of immersion in SBF

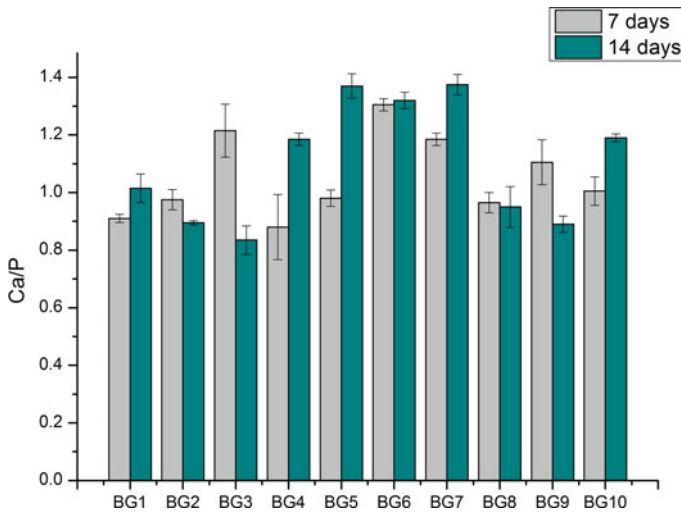


**Fig. 5** Ca/P ratio of the apatite formed for each BG after in vitro test at 7 and 14 days

ALP at 7 and 14 days. Some of them (BG1, BG2, BG3, BG5 and BG6) decreased ALP with SBF exposition time, whereas the opposite behavior was exhibited for the remains BG (BG4, BG7, BG8, BG9 and BG10). These trends are attributed to the different silicon composition employed in each synthesized BG. From CMD, the obtained  $p$ -value  $<0.05$  indicate that silicon represents the highest significance variable on response (growing apatite layer), which is in agreement with previous reported by Hench [5, 14]. That means, large concentrations of silicon reduces any kind of tissue bonding, whereas lower proportions the bonding is promoted highly with soft tissues [5]. In this way, the growing of apatite layer is observed to middle

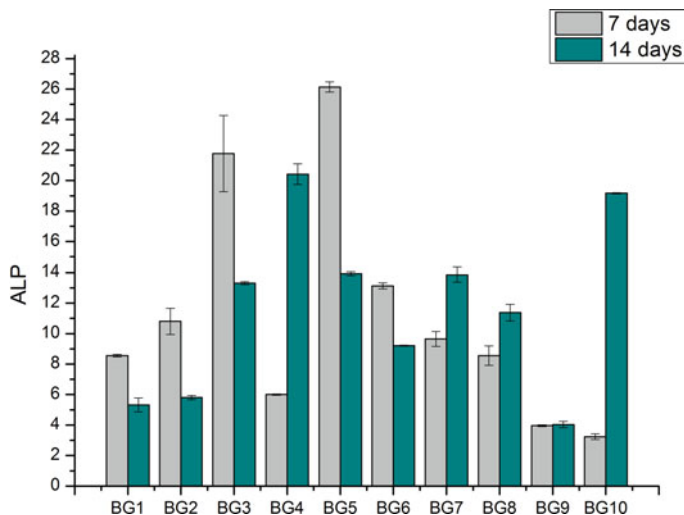


**Fig. 6** Apatite layer percentage of the apatite formed for each BG after in vitro test at 7 and 14 days

combinations of CMD and reduction of this layer for boundary of experimental design.

## Conclusions

In this study, BG were synthesized by sol-gel route at room temperature in a ternary system following a mixture design methodology in order to investigate the role of oxides proportion in apatite layer formation. Considering the results, it has been possible to determine the best result for BG composition for BTE applications according to the design. BG7 composition presented good behavior during in vitro tests with the increase of ALP with SBF exposition time. On the other hand, BG7 was the only one of all synthesized BG that did not present undesirable peaks for some other phases like pseudo-wollastonites on XRD analysis. This confirms that BG7 has the BG typical phase on its structure.

CMD was a useful tool to determine suitable conditions for BG synthesis in order to develop a bioceramic for BTE application with beneficial performance to promote bone like apatite layer formation.

**Acknowledgements** The authors are thankful with Biomaterials Research Group for providing the necessary reagents and studies during the development of this project.

**Conflict of Interest** The authors declare that they have no conflict of interest.

## References

1. Peter, M., Binulal, N. S., Nair, S. V., Selvamurugan, N., Tamura, H., & Jayakumar, R. (2010). Novel biodegradable chitosan–gelatin/nano-bioactive glass ceramic composite scaffolds for alveolar bone tissue engineering. *Chemical Engineering Journal*, 158(2), 353–361. doi:10.1016/j.cej.2010.02.003
2. Catauro, M., Bollino, F., Renella, R. A., & Papale, F. (2015). Sol-gel synthesis of SiO<sub>2</sub>-CaO-P<sub>2</sub>O<sub>5</sub> glasses: Influence of the heat treatment on their bioactivity and biocompatibility. *Ceramic International*, 41(10), 12578–12588. doi:10.1016/j.ceramint.2015.06.075
3. Jones, J. R. (2013). Review of bioactive glass: From Hench to hybrids. *Acta Biomaterialia*, 9(1), 4457–4486. doi:10.1016/j.actbio.2012.08.023
4. Dziadek, M., Zagrajczuk, B., Menaszek, E., Wegrzynowicz, A., Pawlik, J., & Cholewa-Kowalska, K. (2016). Gel-derived SiO<sub>2</sub>-CaO-P<sub>2</sub>O<sub>5</sub> bioactive glasses and glass-ceramics modified by SrO addition. *Ceramic International*, 42(5), 5842–5857. doi:10.1016/j.ceramint.2015.12.128
5. Hench, L. L. (2006). The story of bioglass. *Journal of Materials Science: Materials in Medicine*, 17(11), 967–978. doi:10.1007/s10856-006-0432-z
6. Faure, J., Drevet, R., Lemelle, A., Ben Jaber, N., Tara, A., El Btaouri, H., et al. (2015). A new sol-gel synthesis of 45S5 bioactive glass using an organic acid as catalyst. *Materials Science and Engineering C*, 47, 407–412. doi:10.1016/j.msec.2014.11.045
7. Siqueira, R. L., & Zanotto, E. D. (2013). The influence of phosphorus precursors on the synthesis and bioactivity of SiO<sub>2</sub>-CaO-P<sub>2</sub>O<sub>5</sub> sol-gel glasses and glass-ceramics. *Journal of Materials Science: Materials in Medicine*, 24(2), 365–379. doi:10.1007/s10856-012-4797-x
8. Cornell, J. A. (2002). *Experiments with mixtures: Designs, models, and the analysis of mixture data* (3rd ed.). Hoboken, NJ, USA: Wiley.
9. Kokubo, T., & Takadama, H. (2006). How useful is SBF in predicting in vivo bone bioactivity? *Biomaterials*, 27(15), 2907–2915. doi:10.1016/j.biomaterials.2006.01.017
10. Vaid, C., & Murugavel, S. (2013). Alkali oxide containing mesoporous bioactive glasses: Synthesis, characterization and in vitro bioactivity. *Materials Science and Engineering C*, 33(2), 959–968. doi:10.1016/j.msec.2012.11.028
11. Desogus, L., Cuccu, A., Montinaro, S., Orrù, R., Cao, G., Bellucci, D., et al. (2015). Classical Bioglass<sup>®</sup> and innovative CaO-rich bioglass powders processed by Spark Plasma Sintering: A comparative study. *Journal of the European Ceramic Society*, 35(15), 4277–4285. doi:10.1016/j.jeurceramsoc.2015.07.023
12. Saltzman, W. M. (2009). Biomechanics. In *Biomedical engineering. Bridging medicine and technology* (p. 656). Cambridge University Press.
13. Wu, S., Liu, X., Yeung, K. W. K., Liu, C., & Yang, X. (2014). Biomimetic porous scaffolds for bone tissue engineering. *Materials Science and Engineering R: Reports*, 80(1), 1–36. doi:10.1016/j.mser.2014.04.001
14. Hench, L. L., Splinter, R. J., Allen, W. C., & Greenlee, T. K. (1971). Bonding mechanisms at the interface of ceramic prosthetic materials. *Journal of Biomedical Materials Research*, 5(6), 117–141. doi:10.1002/jbm.820050611

Proceedings of the 3rd Pan American Materials  
Congress

Meyers, M.A.; Benavides, H.A.C.; Brühl, S.P.; Colorado,  
H.A.; Dalgaard, E.; Elias, C.N.; Figueiredo, R.B.;  
Garcia-Rincon, O.; Kawasaki, M.; Langdon, T.G.;  
Mangalaraja, R.V.; Marroquin, M.C.G.; da Cunha Rocha,  
A.; Schoenung, J.; Costa e Silva, A.; Wells, M.; Yang, W.  
(Eds.)

2017, XXV, 816 p. 489 illus., Hardcover

ISBN: 978-3-319-52131-2